Fluid Structure Interaction Induced by Liquid Slosh in Partly Filled Road Tankers

Guorong Yan and Subhash Rakheja

Abstract—The liquid cargo contained in a partly-filled road tank vehicle is prone to dynamic slosh movement when subjected to external disturbances. The slosh behavior has been identified as a significant factor impairing the safety of liquid cargo transportation. The laboratory experiments have been conducted for analyzing fluid slosh in partly filled tanks. The experiment results measured under forced harmonic excitations reveal the three-dimensional nature of the fluid motion and coupling between the lateral and longitudinal fluid slosh at resonance. Several spectral components are observed for the transient slosh forces, which can be associated with the excitation, resonance, and beat frequencies. The peak slosh forces and moments in the vicinity of resonance are significantly larger than those of the equivalent rigid mass. Due to the nature of coupling between sloshing fluid and vehicle body, the issue of the dynamic fluid-structure interaction is essential in the analysis of tank-vehicle dynamics. A dynamic pitch plane model of a Tridem truck incorporated the fluid slosh dynamics is developed to analyze the fluid-vehicle interaction under the straight-line braking maneuvers. The results show that the vehicle responses are highly associated with the characteristics of fluid slosh force and moment.

Keywords—Braking performance, fluid induced vibration, fluid slosh, fluid structure interaction, tank trucks, vehicle dynamics.

I. INTRODUCTION

FLUID slosh within a moving tank is known to be quite complex, particularly under the influence on multiple-axis excitations, as encountered in road tank vehicles. Tank trucks involved in general-purpose transportation of bulk liquids may encounter partial fill conditions due to local regulations on the axle loads and variations in the product weight density. The dynamic slosh forces inside moving road tank vehicles arises from either lateral or longitudinal acceleration fields or a combination of the two during a steering and/or braking maneuver. The magnitudes of transient slosh forces and moments are significantly larger than those derived from the steady-state or quasi-static analysis [1]-[4].

The fundamental properties of transient fluid slosh could be effectively investigated through laboratory experiments under controlled conditions. Such experiments can provide considerable insight into the fluid slosh and associated forces and moments. The majority of the previous experimental investigations on the fluid slosh have been conducted in model tanks which are small in size compared to the full-scale tanks [5]-[8]. Since the similarity of sloshing fluid flows is very complex, the slosh behavior would be expected to differ for different tank sizes. Moreover, difficulty may be encountered when the laboratory experiments are implemented for coupled slosh-vehicle systems.The computational fluid dynamics (CFD) also provides an effective means of predicting the non-linearity of dynamic fluid slosh. The approach has recently gained an increased attention. A number of efforts have contributed to explore feasibility of numerical algorithms for the fluid slosh modeling [9]-[13]. The CFD slosh models were rarely implemented for the fluid slosh analysis in the coupled slosh-vehicle systems, although the incorporation into vehicle models is quite possible. The analyses of coupled fluid-vehicle systems in majority of the studies have considered fluid slosh forces and moments derived from either quasi-static approach [14]-[17] or mechanical analogy method [18]-[21] to ease integration with the vehicle models. Moreover, the analyses have been mostly limited to either the roll plane or the pitch plane, with only a few exceptions [22].
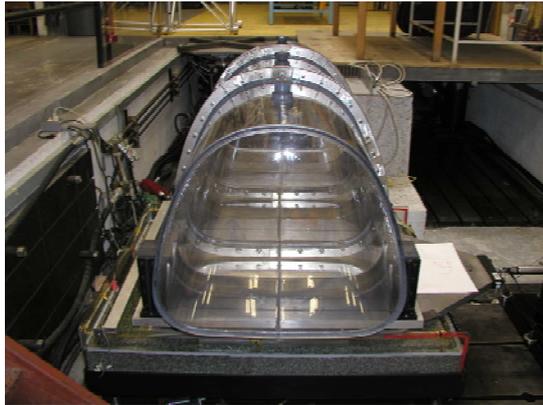
In this paper, the 3-D fluid slosh is experimentally investigated in a relatively large size laboratory tank which can be equipped with baffles. The measured data are analyzed to explore the correlation of slosh characteristics to external excitations. The fluid-vehicle interaction is further investigated employing a coupled tank-truck pitch-plane model subject to straight-line braking maneuvers. The model is formulated by integrating a 3-D CFD fluid slosh model of a partly-filled tank with a 7-DOF pitch-plane model of the vehicle.
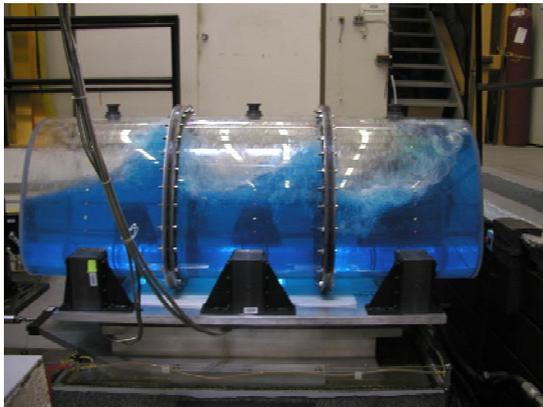
II. FLUID SLOSH EXPERIMENT

The fluid slosh experiments were conducted in laboratory using a scale model tank of cross-section, similar to the "Reuleaux triangle" with variable arc widths, as shown in Fig. 1(a). The tank cross-section was realized on the basis of the optimal tank geometry proposed by Kang et al. [23]. The test tank was designed with total length of 1.85 m, cross-section area of 0.426 m^2 and volume capacity of 760.

G. Yan, Research Engineer, NSERC (Natural Sciences and Engineering Research Council of Canada) IRDF Holder, Life Prediction Technologies Inc., Ottawa, Canada (e-mail: yan.guorongg@gmail.com)

S. Rakheja, Professor, Department of Industrial & Mechanical Engineering, Concordia University, Montreal, Canada (e-mail: rakheja@alcor.concordia.ca).

World Academy of Science, Engineering and Technology
International Journal of Mechanical and Mechatronics Engineering
Vol:4, No:10, 2010

(a)

(b)

Fig. 1 The scale model tank for laboratory fluid slosh experiments:
(a) front view (xz-plane), (b) side view (yz- plane).

The tank design consisted of three modular sections of equal length, such that two baffles could be conveniently inserted between the flanges of the modular sections, as seen in Fig. 1(b). Two different baffle designs were considered: (*i*) single-orifice baffle (245.5 mm diameter orifice); and (*ii*) multiple-orifice baffle with a 101.6 mm diameter orifice at the geometric center and 34 smaller orifices (38.1 mm diameter with centers located 177.8, 241.3 and 368.3 mm from the geometric center). The porosity of the two baffles was approximately 11% of the entire cross-sectional area.

Three 3-axes dynamometers were installed underneath the tank assembly in a triangular manner to measure dynamic forces developed along the longitudinal (*X*), lateral (*Y*) and vertical (*Z*) axes. The movement of the tank was excited using a hydraulic actuator which was controlled by a servo controller (MTS 407). The acceleration and displacement of the platform with the tank were measured using an accelerometer and a linear variable differential transformer (LVDT), respectively. The force, acceleration and displacement signals were acquired using a National Instrument PCI-6036E DAQ board. A total of 11 channels were used for the acquisition of nine force components from three dynamometers, and the platform acceleration and

displacement. The data were acquired at a rate of 256 Hz using the Labview 7.0 software.

The experiments were designed to measure three components of the dynamic force arising from the liquid slosh within the test tank. The test conditions included three fill volumes (30, 50 and 70% of the tank volume) and different amplitudes (0.5, 1, 2 and 3 m/s^2) of harmonic acceleration excitations at various discrete frequencies in 0.5 to 3 Hz range. The data acquired by the three dynamometers were analyzed to determine the resultant slosh forces and moments, derived by subtracting the inertial forces of the tank structure assembly. The acquired data were low-pass filtered using an 8th order Butterworth digital low-pass filter with the cutoff frequency of 6 Hz.

III. TANK VEHICLE MODEL

The straight-line braking of a partly-filled tank truck was simulated for investigating the coupling between fluid and vehicle body. The analyses were conducted employing a pitch-plane model of the vehicle coupled with the fluid slosh forces and moments derived from the three-dimensional dynamic slosh simulations.

A seven-DOF pitch-plane model was formulated for a tridem truck, where the rear three axles are represented by a single composite axle (Fig. 2). The model considers longitudinal, vertical and pitch motions of the sprung mass, vertical motions of the two unsprung masses, and angular motions of the wheels. The floating fluid cargo within the tank is represented by its resultant transient dynamic forces along the longitudinal and vertical axis, and the pitch moment, which are derived from the slosh model and assumed to act on the vehicle sprung mass center of gravity (O_s). The equations of motion describing the longitudinal (x_s), vertical (z_s) and pitch (α_s) motions of the sprung mass can be expressed as:

$$(m_s + m_{uf} + m_{ur} + m_l)\ddot{x}_s = \overline{F}_{xl} - (F_{xbf} + F_{xbr}) - (m_s g + m_l g + \overline{F}_{zl})\alpha_s \tag{1}$$

$$(m_s + m_l)\ddot{z}_s = \overline{F}_{zl} - (F_{zsf} + F_{zsr}) + (m_s + m_l)g \tag{2}$$

$$(I_{yys} + I_{yyl})\ddot{\alpha}_s = \overline{M}_{yl} + F_{zsf}L_f - F_{zsr}L_r - (H_s - z)(F_{xbf} + F_{xbr}) \tag{3}$$

where $\overline{F}_{xl}$, $\overline{F}_{zl}$ and $\overline{M}_{yl}$ are the resultant longitudinal and vertical forces, and pitch moment, respectively, due to the sloshing liquid cargo. The fluid slosh has been modeled in the CFD approach and its validity has been demonstrated using the experimental data obtained for the scale model tank [24]. The slosh parameters computed in the slosh model coordinate system are transformed to the inertial coordinate system of the vehicle to achieve the coupling of fluid and vehicle. F_{xbf} and F_{xbr} are the braking forces developed at the front and rear tire-road interfaces, respectively. Assuming no wheel lockup, the longitudinal braking forces developed on the tire-road contact are derived from the widely used 'Magic Tire Formula' [25]. The sprung mass (m_s) of the vehicle comprises those of the chassis structure and the tank structure. The fluid cargo mass is represented by m_l, and m_{uf} and m_{ur} are the front and rear

World Academy of Science, Engineering and Technology
International Journal of Mechanical and Mechatronics Engineering
Vol:4, No:10, 2010

unsprung masses, respectively. I_{yys} and I_{yyl} are the pitch mass moments of inertia of the sprung mass and the floating cargo. H_s is the height of the sprung mass cg (center of gravity) position at the static state, and L_f and L_r are the longitudinal positions of the front and rear axles, respectively, from the sprung mass cg, as illustrated in Fig. 2. F_{zsf} and F_{zsr} are the vertical forces developed due to the front and rear suspensions, respectively. Assuming linear stiffness and damping properties of the suspension system, the suspension forces are derived from:

$$F_{zsf} = k_{sf}(z_s - L_f\alpha_s - z_{uf}) + c_{sf}(\dot{z}_s - L_f\dot{\alpha}_s - \dot{z}_{uf})$$
$$F_{zsr} = k_{sr}(z_s + L_r\alpha_s - z_{ur}) + c_{sr}(\dot{z}_s + L_r\dot{\alpha}_s - \dot{z}_{ur})$$

(4)

where k_{si} and c_{si} are the stiffness and damping coefficients of the suspension at axle i ($i=f, r$), and f and r refer to the front and lumped rear axles, respectively. z_{ui} is the vertical displacement of the unsprung mass i from its respective static position.

The equations of motion for the unsprung masses, m_{uf} and m_{ur}, describing the vertical motion ($z_{ui}, i=f, r$) can be expressed from the suspension and inertial forces, such that:

$$m_{ui}\ddot{z}_{ui} = F_{zsi} - F_{zti} + m_{ui}g \qquad (i = f, r)$$

(5)

where F_{zti} is vertical force due to tires on the ith axle. Assuming flat road surface and linear properties, it can be expressed as:

$$F_{zti} = k_{ti}z_{ui} + c_{ti}\dot{z}_{ui} \qquad (i = f, r)$$

(6)

where k_{ti} and c_{ti} ($i=f, r$) are the linear tire stiffness and damping coefficients, respectively.
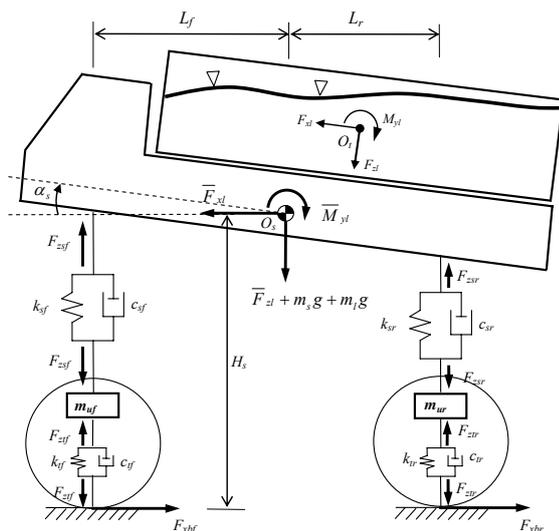

Fig. 2 The seven-degree of freedom (DOF) pitch-plane vehicle model

Fig. 3 illustrates the forces and moments acting on a tire/wheel assembly. Assuming uniform tire-road adhesion and that the braking forces remain below the limit of tire-road adhesion (i.e., no wheel lockup), the angular motion of the wheel/tire combination can be related to the braking force (F_{xbi}) and braking torque (T_i) in the following manner:

$$I_i\dot{\Omega}_i = F_{xbi}R_i - T_i \qquad (i = f, r)$$

(7)

where R_i is the effective rolling radius of wheel i and I_i is the polar mass moment of inertia of the tire-wheel assembly i. The torque distribution is assumed to be proportional to the static normal load on the front and rear axles [26], [27], while the rise time is assumed to be 0.5 s. The driver's reaction time and the braking system time lag are taken as 0.75 s [28], [29]. The braking torque gain of the braking system is set as 98.2 Nm/kPa [29].
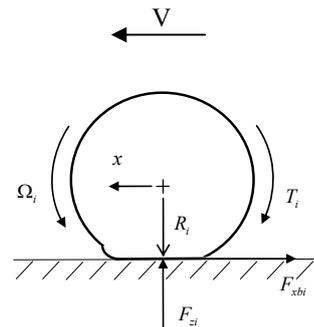

Fig. 3 The model of the tire-wheel assembly

The tridem tank truck considered for the model formulation has 6.65 m wheel base, 3.5 m overall height and 11 m overall length. The gross weight of the truck is approximately 25,840 kg (including the liquid cargo). The sprung mass of the vehicle without the cargo is 5250 kg, while the vehicle full payload capacity is 16,400 kg. The tridem axles are assumed to have the identical properties and responses, and are thus lumped to a single composite axle. Three different liquid products were selected to achieve three different fill volumes but nearly identical cargo load. These included: sulfuric acid, dichloromethane and water, which resulted in fill volume ratios of 38.1%, 52.1% and 69.5%, respectively. The fill heights for the three different fill volumes were 0.63, 0.85 and 1.14 m from the tank bottom. The weight densities of the three fluids were 1826.3, 1326 and 998.2 kg/m^3.

IV. RESULTS AND DISCUSSION

The fluid slosh experiments were conducted subject to external harmonic excitation. The correlation of the fluid responses to the external excitations can be analyzed in terms of frequency and transient forces and moments. Fig. 4 shows the power spectral density (PSD) of measured slosh forces, revealing a number of important spectral components. The results in the figure are derived from slosh forces measured for 50%-filled multiple-orifice baffled tank and cleanbore tank subject to 1 m/s^2 lateral excitation at 0.7 Hz. The two tanks reveal similar magnitudes of the spectral energy of lateral slosh force, while considerable differences is evident for the longitudinal force responses. Two predominant peaks near the

World Academy of Science, Engineering and Technology
International Journal of Mechanical and Mechatronics Engineering
Vol:4, No:10, 2010

excitation frequency ($f_e \approx$ 0.7 Hz) and the lateral mode fundamental frequency ($f_{n,y} \approx$ 1 Hz) are observed in the spectra of lateral force (Fig. 5a). The spectra of the longitudinal slosh force (Fig. 5b) show prominent peaks near the excitation frequency (f_e), longitudinal mode resonant frequency ($f_{n,x} \approx$ 0.45 Hz) and lateral mode frequency ($f_{n,y} \approx$ 1 Hz). This suggests that the variations of transient slosh forces are closely dependent of the external excitation and the slosh resonance. The longitudinal mode resonance of the baffled tank, however, is approximately 1.1 Hz, close to the lateral mode resonance. The higher frequency peaks exhibited in the spectra may be related to higher slosh modes and structural modes.
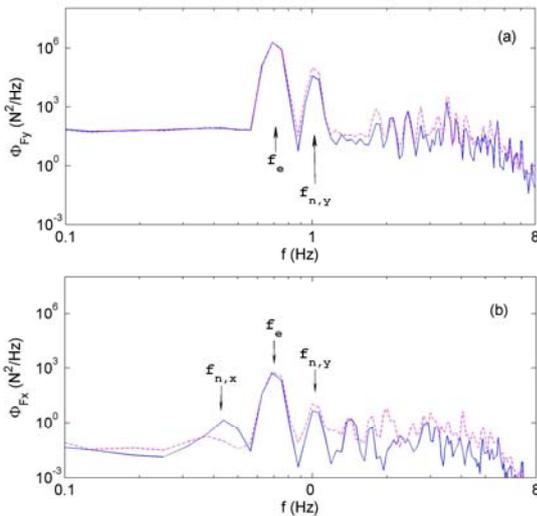
Fig. 5(b) shows that the magnitude of the normalized longitudinal force M_{Fx}, which is the transient peak force divided by the fluid mass. The results reveal that the peak M_{Fx} occurs in the vicinity of the resonant frequency as observed for M_{Fy}, while the peak magnitude tends to increase with the excitation amplitude. The results suggest that the slosh behaves in the two-dimensional manner when the excitation is away from the resonant frequency. A sharp increase in longitudinal force is observed when the excitation approaches the natural frequency, suggesting the presence of 3D swirling motion. The results also show that the maximum force developed in the longitudinal direction is less than 13% of the liquid weight for the given excitations.

Fig. 4 Frequency spectra of slosh force components for 50%-filled tanks subject to the 1 m/s² lateral acceleration excitation at 0.7 Hz: (a) lateral force; (b) longitudinal force. - - - - , cleanbore tank; ——— , tank with multiple-orifice baffles

Fig. 5 illustrates variations in force amplification factors for the 50%-filled cleanbore tank subject to lateral harmonic excitations of different amplitude at various frequencies. The lateral force amplification is derived from the transient peak force divided by the inertial force of the equivalent "frozen" liquid. The responses can thus be interpreted as the amplification factor arising from the dynamic slosh effect. The results in Fig. 6(a) show that the peak amplification factor in lateral force could reach as high as 4. The slosh amplification factor decreases as the excitation amplitude increases, which is attributed to boundary effects. It is interesting to note that the amplification factor approaches a value less than unity at frequencies above 1.4 Hz. This suggests that magnitude of lateral slosh force under excitations at higher frequencies would be considerably smaller than that caused by an equivalent rigid mass. The lower magnitude of lateral force at higher frequency is attributed to relatively smaller magnitude of free surface oscillation. The results do not show peaks in the forces and moments corresponding to higher modes of fluid slosh.
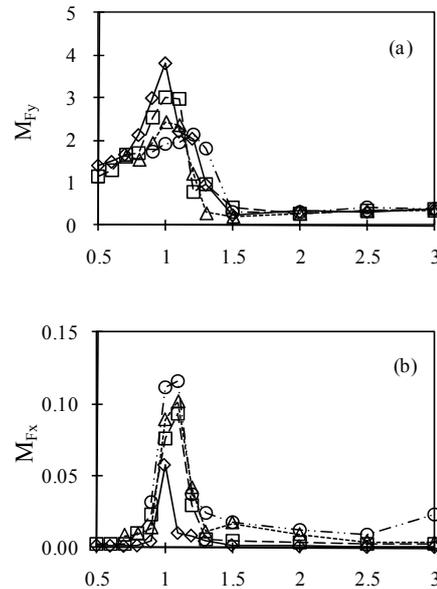

Fig. 5 Normalized slosh force and moment components versus the excitation frequency for 50%-filled cleanbore tank under lateral acceleration excitations (◊, A= 0.5 m/s²; □, A= 1 m/s²; △, A= 2 m/s²; ○, A= 3 m/s². (a) lateral force; (b) longitudinal force.

Fig. 5 also reveals that the maxima of the lateral and longitudinal normalized force components lie in the vicinity of the lateral mode natural frequency ($\approx$1 Hz), irrespective of the excitation amplitude. This confirms that the resonance could induce significantly large slosh force, which should be avoided during the movement of the tank. The simulated responses of a tank truck during a straight-line braking exhibit strong interaction between the fluid cargo and the assembly of tank structure and vehicle body, which can be seen in Figs. 6-8. The simulations were performed under ramp-step treadle pressure considering driver's reaction time and the braking system time lag (0.75s). Fig. 6 illustrates the braking dynamic responses of the coupled vehicle-tank models with and without the baffles (single-orifice) for the 52.1% fill volume. The braking maneuver was synthesized under a 395 kPa treadle pressure on the dry road surface (μ=0.9) with initial vehicle speed of 100 km/h. Fig. 6(a) shows the variations in the pitch angle (α_s) of the sprung mass for both unbaffled and

World Academy of Science, Engineering and Technology
International Journal of Mechanical and Mechatronics Engineering
Vol:4, No:10, 2010

baffled tanks. Fig. 6(b) illustrates the variations in the pitch moment arising from the fluid slosh. The responses reveal a negative pitch angle of the sprung mass, irrespective of the type of cargo and tank configuration indicating a dynamic load transfer to the front axle. The results in Fig. 6(b) show that the sprung mass pitch angle of the cleanbore tank truck tends to oscillate about the steady-state value, while the magnitude decays gradually. In case of the baffled tank, the pitch angle response exhibits only minimal oscillations and the response asymptotically approaches the steady state value. These trends in the pitch response of both baffled and unbaffled tank trucks are closely associated with the slosh pitch moment shown in Fig. 6(a).
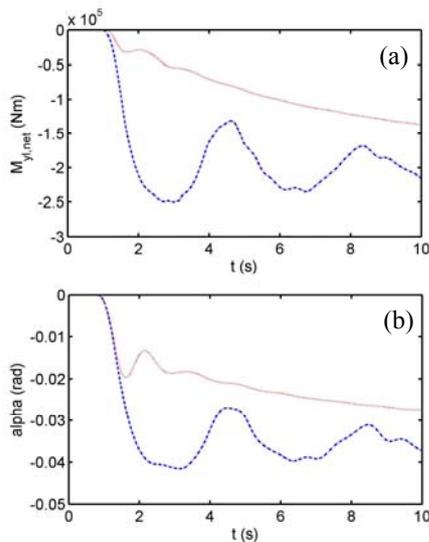

Fig. 6 Transient pitch angle responses of the sprung mass of the vehicle and the transient pitch moment of fluid slosh for baffled and unbaffled tank trucks. ——— , Baffled; - - - - - , Unbaffled

The results in Fig. 6(b) show that the vehicle with a 52.1%-filled cleanbore tank yields significantly larger magnitude of the pitch angle, which oscillates at a frequency of approximately 0.25 Hz, which is identical to that of fluid slosh. This frequency is slightly larger than the fundamental pitch plane slosh frequency (≈ 0.2 Hz) derived from the free oscillations of the fluid within the same tank [24]. It should be noted that the free slosh simulations were performed for the tank fixed at its base, while the tank on a moving truck is subject to the translational and pitch motions. This deviation is most likely attributed to the pitch mode frequency (≈ 1 Hz) of the sprung mass. The fundamental slosh frequency of the baffled tank was obtained near 0.83 Hz, which is also greater than that observed from free slosh within a fixed tank (≈ 0.66 Hz) [24]. These results suggest that the fluid slosh frequency in a tank mounted on a truck is affected by the sprung mass motions and is considerably higher than that derived on the basis of a fixed tank. This further suggests that the fluid slosh within a moving tank necessitates consideration of the coupled tank-vehicle interactions.

The fluid-structure interaction is also observed by comparing the transient vertical slosh force and the vertical bounce motion of the sprung mass. The results in Fig. 7 present that the fluid slosh yields notable vertical force, particularly in the cleanbore tank truck, which yields larger vertical motions of the sprung mass. It is also observed that the vertical responses of the unbaffled tank truck oscillate at a very low frequency near the fundamental slosh frequency (≈ 0.25 Hz), superposed by the bounce mode frequency of the vehicle (≈ 1.1 Hz). The peak vertical force response of the baffled tank truck is significantly smaller than that of the unbaffled vehicle, and it decays rapidly. The results further show that the variations in the vertical responses are quite comparable with those in the vertical force $\overline{F}_{zl}$, which confirms strong interactions between the fluid slosh and the vehicle body dynamics.
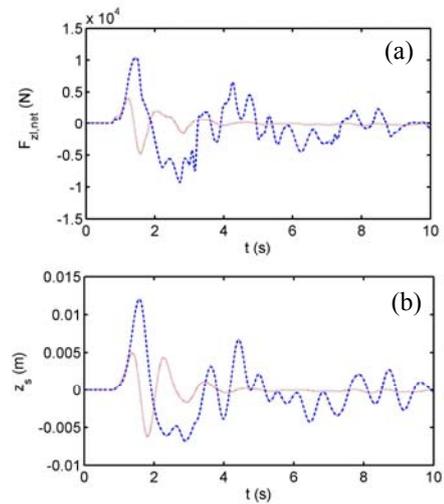

Fig. 7 Transient vertical responses of vehicle body and the vertical force of fluid slosh for baffled and unbaffled tank trucks. ——— , Baffled; - - - - - , Unbaffled
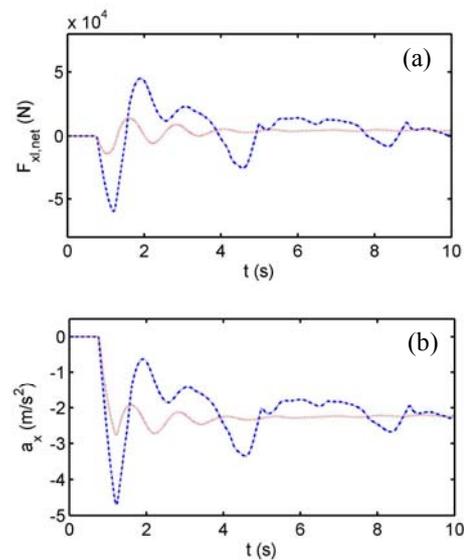

Fig. 8: Longitudinal slosh force ($\overline{F}_{xl}$) and deceleration (a_x) responses of baffled and unbaffled tank trucks. , Baffled; Unbaffled;

World Academy of Science, Engineering and Technology
International Journal of Mechanical and Mechatronics Engineering
Vol:4, No:10, 2010

This coupling effect is also evident from the longitudinal slosh force and vehicle deceleration responses, as shown in Fig. 8. The figure depicts the resultant longitudinal slosh force ($\overline{F}_{xl}$) and vehicle deceleration (a_x) responses under the same conditions. The results show considerably larger magnitudes of the longitudinal slosh force, particularly for the unbaffled vehicle, which consequently deteriorates the deceleration performance of the vehicle. Although the excessive load transfer due to fluid slosh yields relatively larger peak magnitude of deceleration of the unbaffled tank vehicle, the magnitude of the steady state deceleration response tends to be lower. Both the $\overline{F}_{xl}$ and a_x responses of the baffled and unbaffled vehicles oscillate near the respective fundamental slosh frequency, while the presence of baffles yields rapid decay of the oscillations.

V. CONCLUSION

Fluid-structure interactions were investigated in laboratory using a scaled tank subject to external harmonic excitations and studied using a coupled fluid-vehicle model of a partly-filled tank truck for the straight-line braking maneuver.

The experiment results showed that the slosh is a complex phenomenon, containing a number of frequency contents. Predominant peak in the spectrum of a slosh force may occur in the vicinity of the frequency of external excitations. The measured data suggested a coupling between the lateral and longitudinal fluid slosh. The results derived from the coupled tank-vehicle model revealed significant interactions between sloshing fluid cargo and vehicle body. The vehicle vertical and pitch responses are directly related to the vertical slosh force and pitch moment, respectively. The vehicle deceleration response is dependent of the longitudinal dynamic fluid slosh.

ACKNOWLEDGMENT

REFERENCES

[1] C. Winkler, "Rollover of heavy commercial vehicles," UMTRI Research Review, University of Michigan Transportation Research Institute, October-December, 2000, vol.31, no.4.

[2] A.G. Nalecz, and J. Genin, "Dynamic stability of heavy articulated vehicles," Int. J. of Vehicle Design, 1984, vol.5, no.4, pp.417-426.

[3] Kang, X. D., "Optimal tank design and directional dynamic analysis of liquid cargo vehicles under steering and braking," Ph.D. thesis, Department of Mechanical and Industrial Engineering, Concordia University, 2001.

[4] R.D. Ervin, "The influence of size and weight variables on the roll stability of heavy duty trucks," SAE paper, no.831163, 1983.

[5] L. Strandberg, "Lateral stability of Road Tankers", National Road & Traffic Res Inst Report 138A, 1978, Sweden.

[6] H.N. Abramson, W.H. Chu, and D.D. Kana, "Some studies of nonlinear lateral sloshing in rigid containers," Journal of Applied Mechanics, Transactions of the ASME, 1966, vol.33, no.4, pp.777-784.

[7] J.A. Romero, R. Hildebrand; M. Martinez, O. Ramirez and J.M. Fortanell, "Natural sloshing frequencies of liquid cargo in road tankers," Int. J. of Heavy Vehicle System, 2005, vol.12, no.2, pp.121-138.

[8] N. Kobayashi, T. Mieda, H. Shibata and Y. Shinozaki, "A study of the liquid slosh response in horizontal cylindrical tanks," Transactions of the ASME, Journal of Pressure Vessel Technology, 1989, vol.111, February, pp.32-38.

[9] F.H. Harlow and J.E. Welch, "Numerical calculation of time-dependent viscous incompressible flow of fluid with free-surface," Physics of Fluids, 1965, vol.8, no.12, pp.2182-2189.

[10] C.W. Hirt, B.D. Nichols and N.C. Pomeroy, "SOLA – A numerical solution algorithm for transient fluid flows," Los Alamos Scientific Laboratory, Report LA-5852, 1975.

[11] T.C. Su, Y.K. Lou, J.E. Flipse and T.J. Bridges, "A numerical analysis of large amplitude liquid sloshing in baffled containers," Ocean Engineering Program, Texas A&M University, College Station, Texas, USA, Report no. MA-RD-940-82046, 1982.

[12] I. Hadzic, F. Mallon and M. Peric, "Numerical simulation of sloshing, Proc. SRI-TUHH Mini Workshop on Numerical Simulation of Two-phase Flows," Ship Research Institute, Tokyo, Japan, 2001.

[13] P.C. Sames, D. Marcouly and T.E. Schellin, "Sloshing in rectangular and cylindrical tanks," Journal of Ship Research, 2002, vol.46, no.3, Sept., pp.186-200.

[14] S. Rakheja, S. Sankar and R. Ranganathan, "Roll plane analysis of articulated tank vehicles during steady turning," Vehicle System Dynamics, 1988, vol.17, pp.81-104.

[15] R. Ranganathan, S. Rakheja and S. Sankar., "Kineto-static roll plane analysis of articulated tank vehicles with arbitrary tank geometry," Int. J. of Vehicle Design, 1989, vol.10, no.1, pp.89-111.

[16] S. Rakheja and R. Ranganathan. "Estimation of the rollover threshold of heavy vehicles carrying liquid cargo: a simplified approach," Heavy Vehicle Systems, Int. J. of Vehicle Design, 1993, vol.1, no.1, pp.79-98.

[17] S. Rakheja, S. Sankar and R. Ranganathan, "Influence of tank design factors on the rollover threshold of partially filled tank vehicles," SAE paper, No.892480, 1989.

[18] R. Ranganathan, Y. Ying and J.B. Miles, "Analysis of fluid slosh in partially filled tanks and their impact on the directional response of tank vehicles," SAE paper, no.932942, pp.39-45, 1993.

[19] R. Ranganathan, Y. Ying and J.B. Miles, "Development of a mechanical analogy model to predict the dynamic behaviour of liquids in partially filled tank vehicles," SAE paper, no.942307, 1994.

[20] G. Mantriota, "Directional stability of articulated tank vehicles: a simplified model," Heavy Vehicle System, Int. J. of Vehicle Design, 2003, vol.10, nos.1/2, pp144-165.

[21] L. Dai, L. Xu and B. Setiawan, "A new non-linear approach to analysing the dynamic behaviour of tank vehicles subjected to liquid sloshing," Proc. IMechE, Part K: J. Multi-body Dynamics, 2005, vol. 219 pp.75-86.

[22] X. Kang, S. Rakheja, and I. Stiharu, "Cargo load shift and its influence on tank vehicle dynamics under braking and turning", Int. J. of Heavy Vehicle Systems, , 2002. Vol. 9, No. 3, pp.173–203

[23] X. Kang, S. Rakheja, and I. Stiharu, "Optimal Tank Geometry to Enhance Static Roll Stability of Partially Filled Tank Vehicles," SAE Truck and Bus Meeting and Exhibition, Detroit, MI, Nov. 14–17, Proceedings Vol. SP-1486, SAE Paper No. 1999-01-3730, 1999.

[24] G.R. Yan, "Liquid slosh and its influence on braking and roll responses of partly filled tank vehicles," PhD thesis, Concordia University, 2008.

[25] H. Pacejka and E. Bakker, "The magic formula tire model," in Tyre Models for Vehicle Dynamics Analysis, H. Pacejka (ed.), Swets & Zeitlinger, Amsterdam, 1-18, 1993.

[26] D. Cao, S. Rakheja and C.Y. Su, "Pitch attitude control and braking performance analysis of heavy vehicle with interconnected suspensions," SAE paper, 2007-01-1347, 2007.

[27] J.Y. Wong, "Theory of Ground Vehicles,"John Wiley & Sons, Inc., 2001.

[28] P. Delaigue and A. Eskandarian, "A comprehensive vehicle braking model for predictions of stopping distance," Journal of Automobile Engineering, 2004., vol. 218, pp.1409-1417

[29] P.S. Fancher, R.D. Ervin, C.B. Winkler and T.D. Gillespie, "A factbook of the mechanical properties of the components for single-unit and articulated heavy trucks," UMTRI-86-12, The University of Michigan, 1986